

UC Irvine

UC Irvine Previously Published Works

Title

Opsin clines in butterflies suggest novel roles for insect photopigments.

Permalink

<https://escholarship.org/uc/item/4s974105>

Journal

Molecular biology and evolution, 32(2)

ISSN

0737-4038

Authors

Frentiu, Francesca D

Yuan, Furong

Savage, Wesley K

et al.

Publication Date

2015-02-01

DOI

10.1093/molbev/msu304

Peer reviewed

Opsin Clines in Butterflies Suggest Novel Roles for Insect Photopigments

Francesca D. Frentiu,^{†,1,2} Furong Yuan,^{†,2} Wesley K. Savage,^{3,4} Gary D. Bernard,⁵ Sean P. Mullen,³ and Adriana D. Briscoe^{*,2}

¹Institute of Health and Biomedical Innovation, and School of Biomedical Sciences, Queensland University of Technology, Kelvin Grove, QLD, Australia

²Department of Ecology and Evolutionary Biology, University of California, Irvine

³Center for Ecology and Conservation Biology and Department of Biology, Boston University

⁴Department of Biological Sciences, University of Massachusetts, Lowell

⁵Department of Electrical Engineering, University of Washington, Seattle

[†]These authors contributed equally to this work.

*Corresponding author: E-mail: abriscoe@uci.edu.

Associate editor: Stuart Newfeld

Abstract

Opsins are ancient molecules that enable animal vision by coupling to a vitamin-derived chromophore to form light-sensitive photopigments. The primary drivers of evolutionary diversification in opsins are thought to be visual tasks related to spectral sensitivity and color vision. Typically, only a few opsin amino acid sites affect photopigment spectral sensitivity. We show that opsin genes of the North American butterfly *Limenitis arthemis* have diversified along a latitudinal cline, consistent with natural selection due to environmental factors. We sequenced single nucleotide (SNP) polymorphisms in the coding regions of the ultraviolet (*UVRh*), blue (*BRh*), and long-wavelength (*LWRh*) opsin genes from ten butterfly populations along the eastern United States and found that a majority of opsin SNPs showed significant clinal variation. Outlier detection and analysis of molecular variance indicated that many SNPs are under balancing selection and show significant population structure. This contrasts with what we found by analysing SNPs in the *wingless* and *EF-1 alpha* loci, and from neutral amplified fragment length polymorphisms, which show no evidence of significant locus-specific or genome-wide structure among populations. Using a combination of functional genetic and physiological approaches, including expression in cell culture, transgenic *Drosophila*, UV-visible spectroscopy, and optophysiology, we show that key *BRh* opsin SNPs that vary clinally have almost no effect on spectral sensitivity. Our results suggest that opsin diversification in this butterfly is more consistent with natural selection unrelated to spectral tuning. Some of the clinally varying SNPs may instead play a role in regulating opsin gene expression levels or the thermostability of the opsin protein. Lastly, we discuss the possibility that insect opsins might have important, yet-to-be elucidated, adaptive functions in mediating animal responses to abiotic factors, such as temperature or photoperiod.

Key words: *Limenitis*, natural selection, rhodopsin, vision, thermal adaptation, spectral tuning.

Introduction

Vision is made possible by the relationship between opsin genes, which encode opsin proteins, and the chromophore, a light-sensitive, vitamin-derived molecule. The opsin protein binds to the chromophore to form a visual pigment, with key amino acids modulating the absorbance spectra that enable animals to detect particular wavelengths of light (Lythgoe 1979). Diversification of opsin amino acid sites and frequent duplication of this key vision gene have led to the evolution of a variety of visual systems to meet the biological needs of both vertebrates (Yokoyama 2002; Jacobs 2012) and invertebrates (Briscoe and Chittka 2001; Frentiu and Briscoe 2008). The principal selective pressures shaping opsin variation are thought to be the visual light environment, particularly for aquatic organisms, as well as foraging and social signaling to conspecifics and/or predators. For example, in haplochromine cichlid fish, differences in the absorbance spectra of long wavelength-sensitive visual pigments are correlated

with environmental light and, secondarily, male nuptial coloration (Seehausen et al. 2008). Primates have evolved red-green color vision, which can aid in detection of young leaves and ripe fruits (Lucas et al. 2003). *Heliconius* butterflies have evolved duplicate UV-sensitive visual pigments in tandem with wing pigmentation that is UV-yellow which serves as a signal to both conspecifics and predators (Briscoe et al. 2010; Bybee et al. 2012; Finkbeiner et al. 2014).

Diversification of both wing coloration and visual pigments has also occurred among North American admiral butterflies in the genus *Limenitis* (Frentiu, Bernard, Cuevas, et al. 2007). Natural selection for mimetic resemblance between *Limenitis arthemis astyanax* (the red-spotted purple) and its model *Battus philenor* (the pipevine swallowtail) has led to a Batesian mimicry polymorphism within the *L. a. arthemis-astyanax* species complex (Mullen et al. 2008). In addition, Müllerian mimicry has evolved between unpalatable *L. archippus* (viceroy) butterflies and the chemically defended

monarch *Danaus plexippus*. Importantly, genetic and physiological evidence indicates that the visual pigments present in the eyes of *Limnitis* species have diversified spectrally (Frentiu, Bernard, Cuevas, et al. 2007, Frentiu, Bernard, Sison-Mangus, et al. 2007). The eyes of these butterflies have photoreceptors that contain three types of opsins (Pohl et al. 2009), producing long-wavelength (LW), blue (B), and UV light-sensitive visual pigments. The wavelength of peak absorbance (λ_{\max}) of the LW-sensitive visual pigment (LWRh) is distinct in each of these species, with estimates of $\lambda_{\max} = 514$ and $\lambda_{\max} = 545$ nm in the viceroy and the red-spotted purple, respectively.

Although the needs to find food, avoid predators, and engage in social signaling are thought to be the primary drivers of insect opsin diversification, it is unclear whether, and to what extent, natural selection due to abiotic factors varying across geographic landscapes may also contribute. Since the last glaciations, *Limnitis* has expanded its historical range northward along the east coast of North America (Hewitt 2000; Mullen et al. 2011), thereby encountering a steep gradient of day lengths and ambient temperatures that covary with latitude. This provides a unique opportunity to investigate whether natural selection resulting from geographic variation in abiotic factors (Endler 1977) has contributed to opsin diversification by testing for coincident latitudinal clines in opsin sequence variation. Natural selection arising from abiotic factors has been demonstrated to generate the classic clines in phenotypic traits (Coyne and Beecham 1987; Partridge et al. 1994; Schmidt et al. 2005) and gene frequencies (Berry and Kreitman 1993; Schmidt et al. 2008; Fabian et al. 2012) among *Drosophila melanogaster* populations on the east coast of North America.

Here, we report strong clines in genetic polymorphisms at all three opsins in eastern North American *L. arthemis* populations, consistent with the hypothesis that opsin variation has also been shaped by environmental factors that covary with latitude. Analyses of molecular variance (AMOVA) in opsins showed that single nucleotide polymorphism (SNP) variation is explained by balancing selection and exhibits significant signatures of population structure, whereas analyses of neutral markers (amplified fragment length polymorphisms [AFLPs], and the genes *wingless* and *EF-1 alpha*) revealed an absence of population structure. We then comprehensively tested the effect of clinal genetic polymorphisms at key *BRh* opsin amino acid residues on visual pigment λ_{\max} using site-directed mutagenesis, opsin protein expression, UV-visible spectroscopy, and transgenic *Drosophila*. Unexpectedly, we found that blue opsin clinal variation was not correlated with significant differences in visual pigment absorbance spectra. These results suggest that insect opsins, in addition to mediating vision, may play roles in adaptation to the environment, possibly by mediating the effects of temperature and/or the photoperiod.

Results

Clinal Variation in *Limnitis* Opsins

Butterflies were sampled from ten populations on the east coast of the United States (fig. 1; $N = 18$ –38 per population,

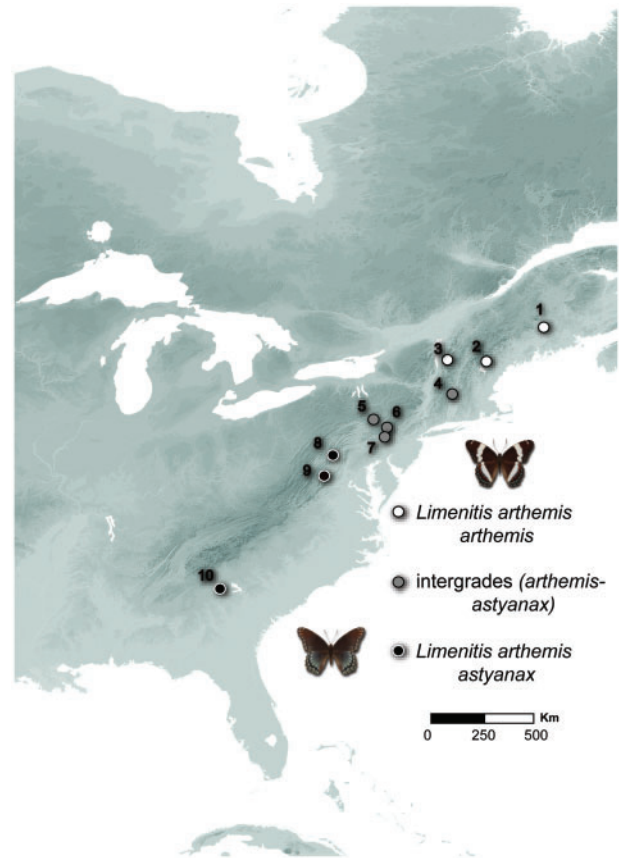


FIG. 1. Geographic locations of *Limnitis arthemis* butterfly populations sampled on the east coast of the United States for nuclear loci SNPs. Localities are: 1. Bangor, ME; 2. Conway, NH; 3. Addison Co., VT; 4. Franklin Co., MA; 5. Columbia Co., PA; 6. Poconos Luzerne Co., PA; 7. Blue Mountains, PA; 8. Allegany Co., MD; 9. Shenandoah Co., VA; 10. Jasper Co., GA.

$N = 249$ total). The total population data set included *L. arthemis arthemis* in the northern part of the distribution and *L. a. astyanax* in the southern part. SNPs present in each population were identified by sequencing coding region fragments of the three opsin genes (*BRh*, *LWRh*, and *UVRh*) expressed in the compound eyes: Exons 1–7 (1,028 bp) of the *BRh* opsin, exons 2–7 (1,192 bp) of the *LWRh* opsin, and exons 2 and 5 (310 bp) of the *UVRh* opsin. Only SNPs that showed variation in at least five populations were further analysed, using weighted logistic regressions for grouped data and with multiple comparisons controlled at a false discovery rate (FDR) of 0.05 (Benjamini and Hochberg 1995). Twelve out of 22 SNPs tested in the *BRh* opsin covaried significantly with latitude, a proxy for abiotic factors that may covary along the geographic gradient (cDNA sites 6, 39, 41, 152, 172, 375, 553, 647, 846, 901, 948, and 972) (supplementary table S1, Supplementary Material online, for regression coefficients and q values). At least 45% of the variation in the frequencies of the 12 SNPs was explained by latitude, and ten were strongly correlated with latitude (pseudo- R^2 values > 0.6 ; fig. 2A). Polymorphisms at six of the 12 sites were nonsynonymous amino acid changes (41: Tyr/Phe; 152: Asn/Ser; 172: Met/Leu; 553: Ile/Phe; 647: Lys/Arg; 901: Thr/Ala). *BRh* opsin SNP

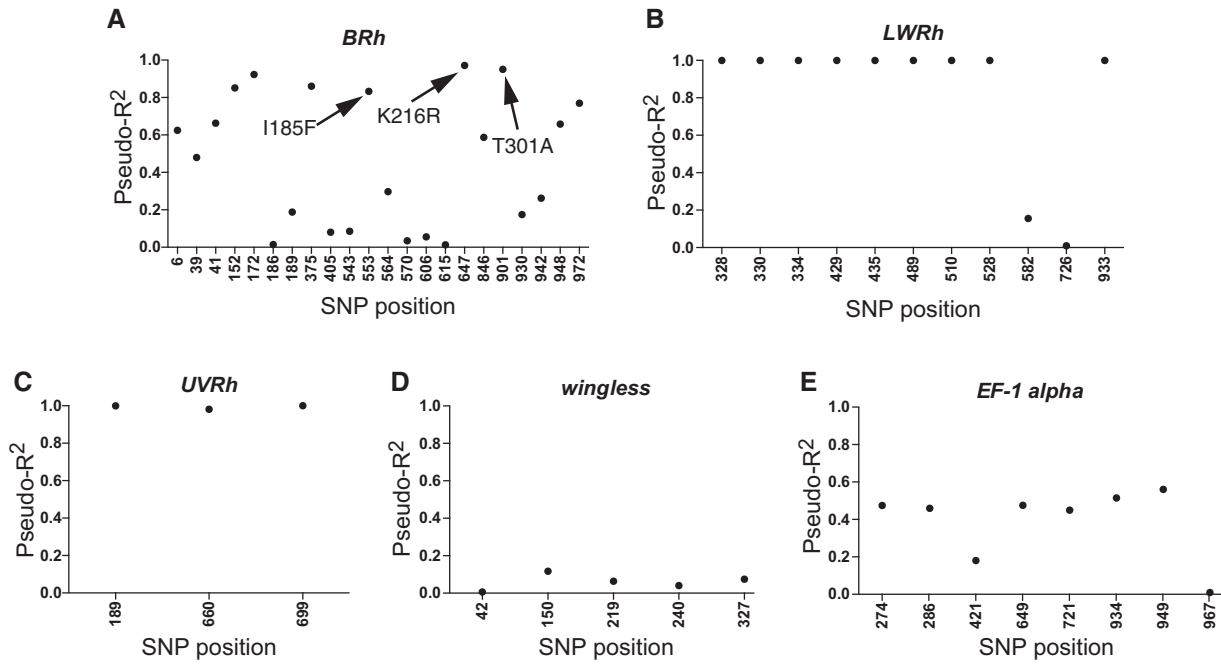


Fig. 2. Latitude explains a large proportion of SNP frequency variation in the *BRh*, *LWRh*, and *UVRh* opsin (A–C) but not *wingless* (D) and *EF-1 alpha* (E) genes. Pseudo- R^2 calculated from weighted logistic regressions for grouped data. Arrows indicate SNPs targeted for site-directed mutagenesis and their encoded amino acid substitutions.

frequencies covaried with latitude in straightforward linear (SNPs 6, 39, 41, 152, 172, 553, 647, 846, 901) and more complex quadratic relationships (SNPs 375, 948, and 972) (supplementary fig. S1, Supplementary Material online). Three SNPs (553, 647, and 901) were located in codons encoding amino acids (185, 216, and 301) that lie within the opsin transmembrane domains. Homology modeling indicated these amino acid sites lie close to the chromophore (supplementary fig. S1, Supplementary Material online, inset). SNP site 647 is equivalent to bovine amino acid site Glu201 with minor (3 nm) spectral tuning effects in vertebrate visual pigments (Nathans 1990).

In the *LWRh* opsin nine of 11 SNPs tested covaried significantly with latitude (*LWRh* opsin cDNA nucleotide sites 328, 330, 334, 429, 435, 489, 510, 528, and 933; supplementary table S1, Supplementary Material online, for regression coefficients and q values). SNP frequencies for all of the sites were highly correlated with latitude, as estimated by pseudo- R^2 values close to 1 (fig. 2B). Nonsynonymous polymorphisms were found at only three sites, two of which share the same codon (328 and 330 Phe/Val; 334 Ala/Ser). All *LWRh* opsin SNPs that varied clinally showed a distinct quadratic relationship with latitude (supplementary fig. S2, Supplementary Material online). Three out of three polymorphic SNPs tested for the *UVRh* opsin covaried significantly with latitude in a linear manner: cDNA sites 189, 660, and 699 (supplementary table S1 and fig. S3, Supplementary Material online). Similar to *LWRh* opsin sites, pseudo- R^2 values were close to one, indicating a very strong relationship between SNP frequencies and latitude in the three *UVRh* sites (fig. 2C). All *UVRh* opsin polymorphisms were silent substitutions. We also sequenced two putatively neutrally evolving genes,

wingless (402 bp) and *EF-1 alpha* (1,066 bp). None of the five SNPs tested for *wingless* varied clinally (fig. 2D and supplementary fig. S4, Supplementary Material online) but six of eight polymorphisms (all silent substitutions) in *EF-1 alpha* covaried significantly with latitude, although with much lower correlations than for the opsins (fig. 2E and supplementary fig. S5, Supplementary Material online).

Genomic Analysis of Population Structure

Next, we used an expanded set of 20 populations of butterflies from the central and eastern United States to examine population structure at the genome-wide level by performing an AFLP analysis (supplementary fig. S6 and table S2, Supplementary Material online). A total of 2,723 AFLP loci were identified, of which 490 had a minor allele frequency ≥ 0.10 and were retained for subsequent analyses (supplementary table S3, Supplementary Material online). To identify loci potentially under selection, Bayesian and frequentist outlier analyses were conducted using the programs BAYESCAN v. 2.0 (Foll and Gaggiotti 2008) and Mchaza (Antao and Beaumont 2011), respectively. Because both approaches resulted in qualitatively similar results (supplementary fig. S7, Supplementary Material online), we focused on results from the Bayesian method. All loci showing $\log(\text{Bayes factor}) > 2$, and $P([\alpha_i \neq 0]) > 0.99$ were retained as outliers potentially under selection (Foll and Gaggiotti 2008). We then partitioned the AFLPs into two sets used for subsequent analyses: 1) all loci (F -statistic [F_{ST}]_a) and 2) neutral loci (F_{ST} _n). Population differentiation estimated using standard F_{ST} was substantial ($F_{ST} = 0.21$) (supplementary table S4, Supplementary Material online). However, F_{ST} calculated based on

dominant markers typically overestimate structure (Bierne et al. 2013). When we partitioned these data into outlier ($N=66$; $FDR=0.001$) and nonoutlier ($N=424$) loci, we found low overall population differentiation (F_{ST} neutral = 0.09 vs. 0.51 for outliers) (supplementary table S4, Supplementary Material online). An AMOVA of the AFLP data calculated in Arlequin v. 3.5 (Excoffier and Lischer 2010) indicated a lack of population structure concordant with wing pattern differentiation ($P=0.471$).

In contrast, AMOVA of sequence data indicated substantial structuring among populations at the three opsin genes but not *wingless* or *EF-1 alpha*. Although most genetic variation was found within populations (51.3–98.0% across the five gene data sets; supplementary tables S5 and S6, Supplementary Material online), high and significant F_{ST} estimates for the opsin genes suggested significant structuring of populations within geographic clusters. The analysis suggested that populations differed among smaller geographic clusters (e.g., grouping populations from ME, NH, and VT; supplementary table S2 and fig. S6, Supplementary Material online), suggesting the population structure evident in opsins was correlated with clinal variation in SNPs. Although regional populations differed, the larger genetic differences occurred among populations with larger geographic distances (supplementary table S6, Supplementary Material online). In contrast, almost all genetic variation ($>97\%$) in *wingless* and *EF-1 alpha* was found within populations rather than among populations (supplementary table S5, Supplementary Material online).

We used the hierarchical island model method developed by Excoffier et al. (2009) in Arlequin v. 3.5 to identify opsin SNPs potentially under selection along the clinal gradient, as well as the type of selection maintaining this genetic variation. Using this outlier approach we identified 47 candidate SNPs for the *BRh* opsin, although using a more stringent criterion of statistical significance ($P < 0.001$) reduced this number to 23 (supplementary table S7, Supplementary Material online). The 12 SNPs found to covary significantly with latitude above were also found to be under selection with this analysis ($P < 0.001$; supplementary table S7, Supplementary Material online). The SNPs detected were most likely under balancing selection as the ratio of F_{ST} to H (heterozygosity) was well outside of the simulated distribution and exceedingly low (below the 1% quantile). Four SNPs were detected as outliers putatively under selection in the *LWRh* opsin gene, only one of which was highly significant ($P < 0.001$; supplementary table S7, Supplementary Material online). None of these four SNPs also covaried significantly with latitude. No outliers were detected for *UVRh* and only marginally significant ones for *wingless* and *EF-1 alpha*, with one exception (supplementary table S7, Supplementary Material online).

A Stable Cell Line System for Expression of *Limenitis* BRh Visual Pigments

To test the effect of variation at key sites in the BRh opsin on the wavelength of peak absorbance, λ_{max} we developed, to our knowledge, the first stable cell culture system for the

expression of insect visual pigments. A stable cell line expressing BRh opsin protein circumvents the disadvantage that transient transfection typically yields protein levels that are too low for accurate measurement of dark spectrum λ_{max} . The *BRh* opsin gene of *L. a. astyanax* (GenBank Accession: AY918902) was cloned into the pGEM-T Easy vector (Promega, Madison, WI) and a short oligonucleotide sequence encoding the 1D4 epitope of bovine rhodopsin (STTVSKTETSQVAPA) was added in-frame to the 3'-end before the stop codon. Tagged sequences were subcloned into the expression vector pcDNA3.1(+) (Invitrogen, Carlsbad, CA), and plasmids were then transfected into vertebrate human embryonic kidney (HEK) 293 cells using Lipofectamine 2000 (Invitrogen) and grown in the presence of the drug G418 sulfate. Eight to 12 cell clones per construct were expanded and screened for BRh opsin expression using western blots (supplementary fig. S8A, Supplementary Material online) and the clone having the highest expression level was selected for further studies. The cultured cells were incubated with 11-*cis*-retinal in the dark. The reconstituted BRh visual pigments were extracted under dim red light, purified and their absorption spectra measured in a Hitachi U-3310 UV-Vis spectrophotometer at 15°C. Using our stable cell culture expression system, we found that the *L. a. astyanax* BRh visual pigment λ_{max} was 430.9 ± 0.03 nm (fig. 3A).

BRh Visual Pigment Validation Using Transgenic *Drosophila*

To validate the results from the stable cell line culture system described above, we constructed transgenic *D. melanogaster* expressing the *L. a. astyanax* BRh visual pigment in photoreceptor cells. The 1D4 epitope-tagged B opsin gene construct above was placed under the control of the *Drosophila* Rh1 opsin promoter and introduced, by P-element mediated germline transformation via embryonic injection, into the genome of *ninaE*¹⁷ mutant flies, which contain a large deletion in the *Rh1* gene resulting in less than 1% of wild-type *Rh1* mRNA (O'Tousa et al. 1985). After repeatedly inbreeding the transformed fly lines to generate individuals homozygous for each opsin transgene, transgenic animals were screened for protein expression in the R1-6 photoreceptor cells using the 1D4 antibody on sectioned eyes and visualized using light microscopy (supplementary fig. S9A and B, Supplementary Material online). Transgenic fly lines were screened for the presence of the *Limenitis* BRh transgene by polymerase chain reaction (PCR), sequencing and western blot (supplementary fig. S9C, Supplementary Material online). The BRh visual pigment was purified from *Drosophila* eyes (see Materials and Methods) and its absorbance spectra measured. We found that *L. a. astyanax* BRh opsin expressed in *Drosophila* had a λ_{max} of 427.6 ± 0.17 nm (fig. 3A, inset), in close agreement with the estimate obtained from the cell culture expression system.

We also measured the action spectra of the pupillary response in living *Drosophila* ($N=3$) expressing the *L. a. astyanax* BRh visual pigment in the R1–R6 photoreceptor cells.

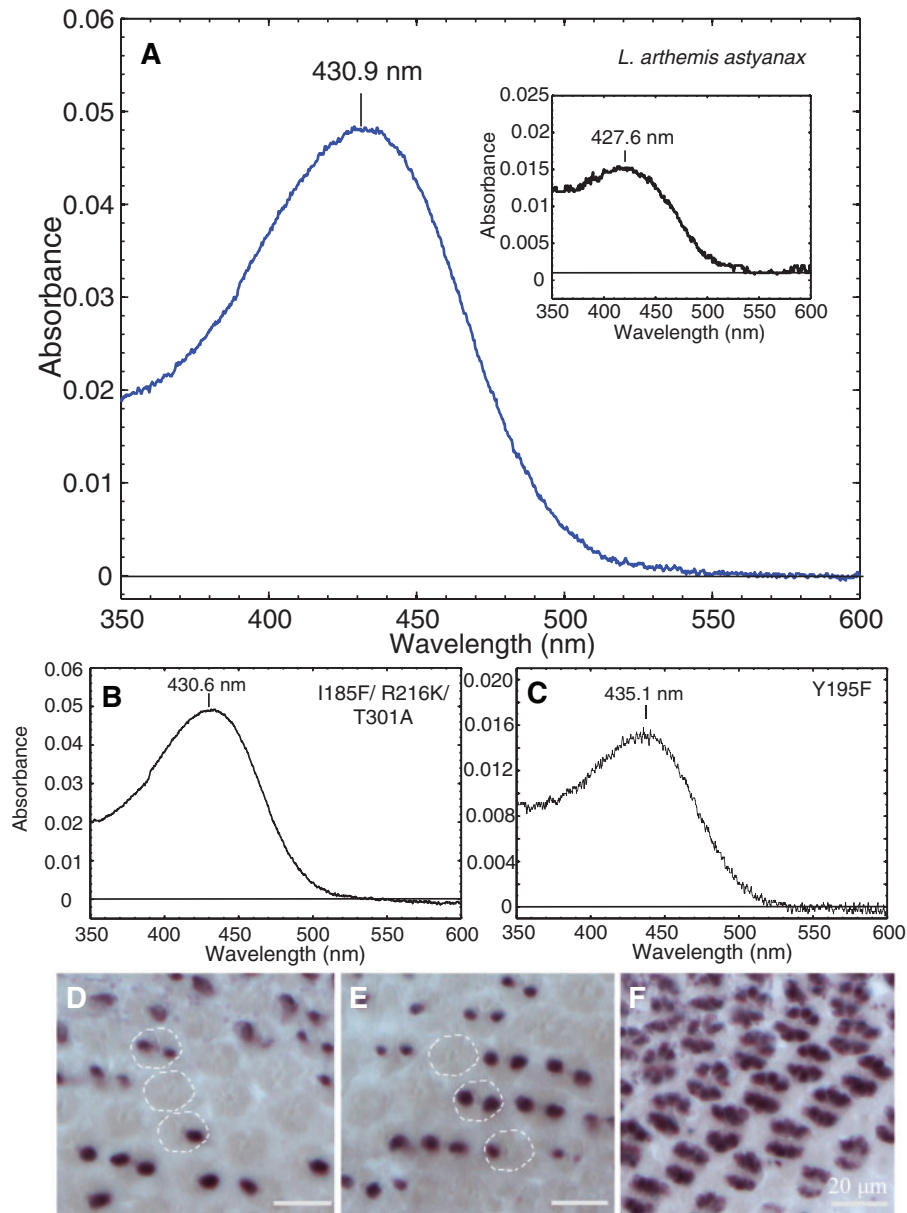


Fig. 3. Dark spectrum of *Limenitis a. astyanax* BRh native and mutant photopigments expressed using an HEK293 stable cell culture system and opsin mRNA expression in the main retina of adult *L. a. astyanax*. (A) Native *L. a. astyanax* BRh rhodopsin, $\lambda_{\max} = 430.9 \pm 0.03$ nm. Estimates of λ_{\max} were made by least-squares fitting of the data to a visual pigment template of (Stavenga et al. 1993). Inset: Dark spectrum of *L. a. astyanax* BRh rhodopsin purified from *Drosophila melanogaster* eyes, $\lambda_{\max} = 427.6 \pm 0.17$ nm. (B) Triple mutant pigment for clinically varying SNPs encoding I185F, K216R, and T301A amino acid substitutions, $\lambda_{\max} = 430.6 \pm 0.05$ nm. (C) Y195F mutant, $\lambda_{\max} = 435.1 \pm 0.06$ nm, a positive control with known spectral tuning effects in butterfly photopigments (Wakakuwa et al. 2010). (D–F) (D) Tangential section of an adult butterfly eye showing *UVRh* mRNA in R1 and R2 photoreceptor cells. (E) Adjacent section to (D) showing *BRh* mRNA in R1 and R2 photoreceptor cells where *UVRh* is not expressed. (F) Tangential section showing *LWRh* mRNA expression in R3–8 photoreceptor cells.

The measurements indicated the presence of a visual pigment with a λ_{\max} of 427.0 ± 1.6 nm (95% CI = 424–430 nm) (supplementary fig. S10A, Supplementary Material online), in good agreement with the estimate obtained by purifying the *L. a. astyanax* BRh opsin expressed in *Drosophila* and the stable cell culture system.

Epi-Microspectrophotometry of *L. a. astyanax* Eyes

As an additional control to the stable cell line expression system and to confirm BRh peak absorbance in adult *L. a.*

astyanax eyes, we bleached the LWRh visual pigment of a completely intact adult male butterfly and measured eyeshine reflectance with dim monochromatic flashes of 5-nm bandwidth, from 380 to 750 nm every 10 nm. Densitometric analysis (Briscoe et al. 2003; Yuan et al. 2010) revealed round-trip densities 0.30 of R545 and 0.32 of metarhodopsin M490. Stripping R544 and M490 created a residual fit by density 0.67 of R435 (supplementary fig. S10B, Supplementary Material online). We estimated the $\lambda_{\max} = 434.8$ nm \pm 0.5 nm using a least squares fit to the visual pigment template of

(Palacios et al. 1996). Our measurement for the native BRh visual pigment in vivo is consistent with estimates obtained from both the stable cell culture system and transgenic *Drosophila*.

Effect of BRh Opsin SNPs on Visual Pigment Absorbance Spectra

All three methods of measuring BRh visual pigment λ_{\max} yielded estimates that were in very close agreement. Therefore, we used the HEK293 cell culture system to test the effects of several nonsynonymous selected SNPs on visual pigment spectral tuning. In particular, we focused on the 553, 647, and 901 SNP sites that encode amino acids close to the chromophore and that may affect visual pigment absorbance spectra. Site-directed mutagenesis in the *L. a. astyanax* background indicated that the 553 site (I185F) (supplementary fig. S11A, Supplementary Material online) had no impact on λ_{\max} , whereas the 647 site (K216R) produced a small 2 nm blue-shift ($\lambda_{\max} = 428.6 \pm 0.04$ nm) (supplementary fig. S11B, Supplementary Material online). A T301A substitution comprising site 901 produced an even smaller 1 nm blue-shift ($\lambda_{\max} = 429.8 \pm 0.06$ nm) (supplementary fig. S11C, Supplementary Material online). The triple mutant I185F/K216R/T301A produced no significant impact on λ_{\max} (compare fig. 3A with 3B). As a negative control, we mutated the lysine in the chromophore-binding site, K325A, which destroyed the absorbance spectrum of the photopigment altogether (supplementary fig. S11D, Supplementary Material online). As positive controls, we expressed the monarch *D. plexippus* BRh (Genbank Accession: AY605544) and measured a $\lambda_{\max} = 438.9 \pm 0.04$ nm, which was very similar to the spectral sensitivity maximum of in vivo intracellular photoreceptor recordings ($\lambda_{\max} = 435$ nm) (supplementary fig. S11E, Supplementary Material online; Stalleicken et al. 2006), along with the BRh of the viceroy, *L. archippus* ($\lambda_{\max} = 431.1 \pm 0.08$ nm) (Genbank Accession: EU358777) (supplementary fig. S11F, Supplementary Material online). We also introduced a Y195F substitution at a known insect opsin spectral tuning site (Wakakuwa et al. 2010) into the native *L. a. astyanax* opsin by site-directed mutagenesis and produced a pigment that is red-shifted by approximately 4 nm ($\lambda_{\max} = 435.1 \pm 0.06$ nm) (supplementary fig. 3C, Supplementary Material online), which is the same magnitude of effect in other butterfly photopigments. In summary, our experiments provide strong evidence for a lack of a biologically significant spectral tuning effect of clinally varying SNPs in the blue opsin of *L. arthemis*.

Using in situ hybridizations of adult *L. a. astyanax* eyes, we found that, like in other nymphalid butterflies (Sauman et al. 2005), the *UVRh* and *BRh* mRNAs were localized in R1 and R2 photoreceptor cells in the main retina and form three subtypes of ommatidia (UV-UV, UV-B, and B-B). The *LWRh* mRNA was localized to the R3-8 photoreceptor cells (supplementary fig. 3D–F, Supplementary Material online). Taken together, these data indicate that *BRh* is the locus encoding the blue-sensitive visual pigment.

Discussion

Opsins are ancient molecules that enable the critical task of animal vision. The diversification of opsins is generally thought to be driven by selection on visual pigments from different light environments or for color vision. Color vision requires visual input from at least two spectrally distinct photoreceptors and, in butterflies, is critical for mate recognition and foraging. Our discovery of clines in *Limnitis* opsin genes along the east coast of North America strongly suggests that diversification of these molecules has also been driven by selection due to abiotic factors that covary with latitude. Interestingly, a recent genome-wide survey of *D. melanogaster* has also shown evidence of clines in the opsins *Rh1*, *Rh5*, *Rh6* and *Rh7* along the same geographic region (see supplementary tables S5, S7, and S8, Supplementary Material online and clinal plots for NinaE_FBgn0002940, Rh5_FBgn0014019, Rh6_FBgn0019940 and Rh7_FBgn0036260 in Appendix S14 of Fabian et al. [2012]), indicating that these clines are likely maintained by natural selection rather than demography. Similar to this result, our analysis of genome-wide patterns at putatively neutral AFLPs supports this scenario for *Limnitis*: The absence of significant genetic structure among populations suggests that opsin clines are not due to demographic factors.

We found clinal genetic variation in all three opsins that are known to encode for visual pigments in *Limnitis*. Most strikingly, a large number of *BRh* opsin polymorphic sites encoding nonsynonymous amino acid substitutions covaried with latitude to a significant extent, indicating the action of natural selection on this molecule. The same sites strongly covarying with latitude were found to be under balancing selection in a separate analysis that only considers molecular patterns of population structure. Evidence of balancing selection strongly suggests that the SNP diversity is maintained in populations because they are advantageous. However, only three out of 12 sites encoding amino acid substitutions are located close to the chromophore, suggesting that most sites that varied clinally are unlikely to influence spectral tuning. Using a novel stable cell line system, transgenic *Drosophila*, and site-directed mutagenesis, we also showed that these three sites, which are located close to the chromophore and vary clinally, have almost no effect on spectral tuning. In contrast to the *BRh* opsin, all clinally varying *LWRh* SNPs covaried strongly with latitude in a nonlinear manner. The majority of clinally varying *LWRh* SNPs comprised silent substitutions, but three SNPs led to nonsynonymous changes. Interestingly, one SNP (site 334) encoded a Ser-to-Ala substitution that has previously been inferred to be under selection using a branch-site test ((Frentiu, Bernard, Cuevas, et al. 2007), amino acid site 91). The site also has small spectral tuning effects in the squid retinochrome (Terakita et al. 2000).

We note that in addition to the nonsynonymous SNPs that vary clinally in the opsins, our analyses reveal a number of synonymous SNPs that exhibit similar patterns of variation. In *BRh*, three of these six synonymous SNPs (6, 39, and 846) are in the same exons as, and in close proximity to, two selected nonsynonymous SNPs (41 and 901). Similarly,

in *LWRh* five of six synonymous SNPs (429, 435, 489, 510, and 528) are located in an exon that is separated by a very small (83 bp) intron from an exon containing the three-selected nonsynonymous SNPs (328, 330, and 334). The close proximity of most synonymous and nonsynonymous SNPs that vary clinally suggests that these synonymous SNPs are not likely to be under selection themselves but instead are causally linked to nonsynonymous SNPs that are the direct targets of selection. The fact that they exhibit similar patterns of clinal variation is because recombination has not yet broken apart their association.

The significance of the remaining synonymous SNPs (e.g., those in the *UVRh* gene) that are not in close proximity to potentially selected nonsynonymous SNPs remains unclear. A number of studies have shown that selection can act on synonymous sites affecting thermodynamic stability or translational efficiency of mRNA (Shields et al. 1988; Cuevas et al. 2011; Shabalina et al. 2013). Synonymous sites may also be the targets of regulation of gene expression via noncoding or micro RNAs (Mercer et al. 2009; Schnall-Levin et al. 2010). A number of noncoding RNAs that are antisense to introns have been identified, possibly regulating splicing (He et al. 2008). It is therefore possible that some of these clinally varying synonymous sites or sites that they are linked to may impact other aspects of opsin biology such as gene expression levels. If so, such differences in gene expression should they exist might have a significant impact on visual sensitivity of the animals but not on their spectral tuning. Finally, some of these synonymous SNPs may be, despite our FDR correction, false positives. We note that the SNPs that vary clinally in the *Drosophila* opsins are mostly in noncoding parts of the genes and include intronic substitutions and substitutions in the 5'-UTR, upstream, and downstream genomic regions of the opsins (Fabian et al. 2012; supplementary table S7, Supplementary Material online, Daniel K. Fabian, personal communication). The two clinally varying SNPs in the opsin-coding regions are a nonsynonymous substitution in *Rh6* and a synonymous substitution in *Rh2* (See FP comparison of Fabian et al. [2012]). The fact that the opsins of both *Limenitis* and *Drosophila* represent targets of spatially varying selection along the same geographical range suggests that differentiation at these loci is unlikely the result of demography alone.

Latitudinal clines generally result from adaptation to climatic factors that vary in a consistent manner, in particular temperature (Partridge et al. 1994; Hoffmann et al. 2002). Recent work with *Drosophila* has shown that rhodopsins can also mediate some temperature-based responses, particularly in larvae (Shen et al. 2011), via an unknown mechanism. A large number of genes are known to be involved in thermal adaptation, for example metabolism genes, heat shock proteins, and pigmentation genes. We suggest that opsins, classic vision molecules not traditionally thought to be involved in thermoregulation, may be implicated in adaptation to temperature in insects. Some of the clinally varying nonsynonymous SNPs in the BRh opsin that have no effect on spectral tuning, for example, may instead play a role in the thermostability of the opsin protein.

Opsins may also behave like other light- and temperature-sensitive molecules involved in circadian clocks. For example, the gene *timeless*, involved in the clock cycle, shows latitudinal variation and may be sensitive to seasonal day length and temperature, which covaries with latitude (Sandrelli et al. 2007). Photoperiod is a predictable environmental cue that can be used to respond to seasonal variation, and latitudinal clines in light-sensitive molecules may have evolved to enable measurement of this critical parameter (Hut et al. 2013). An important photoperiodic response in insects is diapause (Leather et al. 1993) and, in North American *D. melanogaster* populations, its incidence is positively correlated with increasing latitude (Schmidt et al. 2005). As *Limenitis* radiated from south to north (Mullen et al. 2011), it too has encountered high variability in temperatures and day lengths. Therefore, it is possible that opsins may be involved in adaptive responses to both of these factors—light and temperature—perhaps mediated by thermostability of opsin mRNAs or proteins or both, together with the light sensitivity of the photopigment.

Lastly, we found that SNPs covaried in both linear and quadratic manners with latitude, indicating that the pattern of opsin genetic variation present in *Limenitis* populations is complex. Nonlinear clines have been previously reported for a range of traits in *Drosophila*, where clines have been most thoroughly studied. These include cuticular hydrocarbons (Frentiu and Chenoweth 2010) and body size in *D. melanogaster* (James et al. 1995) and heat tolerance in *D. simulans* (van Heerwarden et al. 2012). The nonlinear component of the cline in many SNPs appears to be at the southern end of the distribution of the species (supplementary figs. S1 and S3, Supplementary Material online). The pattern may be due to nonlinear variation in abiotic factors and/or other biotic factors that are shaping variation in opsins. For example, southern populations experience contact with the model butterfly *B. philenor* (the pipevine swallowtail). These populations of *L. a. astyanax* also have striking blue iridescent wing colors, potentially resulting in differential selection pressures among different butterfly populations.

In conclusion, our data suggest that besides mediating color vision, insect opsins may have additional roles in adaptive responses to environmental factors, which may also drive the evolution of these molecules. Clines are generally thought to represent selection due to abiotic factors that covary with latitude. Therefore, opsin evolution may be constrained by antagonistic sources of natural (abiotic, predation) and sexual (mate choice, social signaling) selection.

Materials and Methods

Sample Collection and Opsin DNA Sequencing

Butterflies were collected as adults in the field from ten locations along an eastern transect (fig. 1): Bangor, ME (latitude 44.0861°) (N individuals = 23); Conway, NH (44.0536°) (N = 39); Addison Co., VT (44.0495°) (N = 24); Franklin Co., MA (42.5808°) (N = 21); Columbia Co., PA (41.3788°) (N = 22); Luzerne Co., PA (41.1022°) (N = 24); Carbon Co., PA (40.7658°) (N = 24); Allegany Co., MD (39.6242°) (N = 20); Shenandoah Co., VA (38.8828°) (N = 27); Jasper

Co., GA (33.3066°) ($N = 25$). *BRh* opsin for the MA population and *LWRh* opsin sequences for the GA population were directly sequenced from RT-PCR products amplified from Trizol-extracted total RNA from the eyes of adult butterflies. For all other populations, DNA was extracted using the DNeasy kit (Qiagen), amplified via PCR using gene-specific primers (supplementary table S8, Supplementary Material online) and sequenced using BigDye chemistry v3.1 (Applied Biosystems, Inc.) at the UC Irvine DNA Core.

Analyses of Neutral Markers

We used an expanded set of butterflies ($N = 417$ individuals) for AFLP genotyping, with individuals collected from 20 localities (14–24 individuals per site). Genomic DNA was isolated from flight muscle tissue using the DNeasy kit (Qiagen, Inc.), quantified by spectrophotometry, and standardized to working concentrations of 100 ng/ μ l. We used the ABI Small Genome Mapping Kit (Applied Biosystems) to genotype all individuals with 12 selective AFLP primer combinations (supplementary table S3, Supplementary Material online). A 4 μ l of a 1:4 dilution of selective amplification product was prepared for each sample, which was then added to 8 μ l formamide with 1.25% GeneScan ROX-500 size standard (Applied Biosystems). AFLP fragments were separated using an ABI 3730 automated sequencer and scored and assigned to bins using ABI GENEMAPPER software version 3.7. Scored fragments ranged in size from 100 to 500 bp and had a minimum fragment signal intensity, measured as relative fluorescent units, of 150.

To identify potential AFLP loci under selection, we conducted outlier analyses using two distinct approaches. First, we used the frequentist approach implemented in Mcheza (Antao and Beaumont 2011), which utilizes coalescent simulations to generate a null distribution of neutral F_{ST} values. Mcheza provides a correction that accurately approximates F_{ST} even when the number of demes is very low and allows for multitest correction based on FDRs (Chiurugwi et al. 2011). We also employed a Bayesian method to estimate directly the posterior probability that each locus is subject to selection using the program BAYESCAN v. 2.0 (Foll and Gaggiotti 2008). The Bayesian approach takes all loci into account in the analyses through the prior distribution, resolving the problem of multiple testing of a large number of genomic locations. Within BAYESCAN, the estimation of model parameters was automatically tuned on the basis of short pilot runs (ten pilot runs, length 5,000), using the default chain parameters in the program: The sample size was set to 5,000 and the thinning interval to 20. All loci showing $\log(\text{Bayes Factor}) > 2$, and also $P([\alpha_i \neq 0] > 0.99)$ were retained as outliers, which provides decisive support for accepting the model (Foll and Gaggiotti 2008). Both methods of outlier detection performed similarly so we focused our inferences on the results of the combined Bayesian analysis.

HEK293 Cell Culture Expression, Reconstitution, and UV-Visible Spectroscopy of BRh Visual Pigments

Total RNAs were extracted from single adult butterfly heads using Trizol (Invitrogen). cDNAs were then synthesized using

a Marathon cDNA amplification kit (BD Biosciences, Franklin Lakes, NJ). The *BRh* coding regions of different *Limenitis* species were amplified using proof-reading BD *Taq* polymerase (BD Biosciences), cloned into pGEM-T easy vector (Promega). A short oligonucleotide sequence encoding the 1D4 epitope of bovine rhodopsin (STTVSKTETSQVAPA) was added in-frame to the 3'-end before the stop codon. The tagged cDNA fragments were then subcloned into expression vector pcDNA3.1(+) (Invitrogen). Site-directed mutations were made using proof-reading BD *Taq* DNA polymerase. Transient transfection of plasmid DNA was carried out by Lipofectamine 2000 (Invitrogen). For each transfection, 3 μ g of plasmid DNA was used on one 6-cm dish of HEK 293. The cells were replated 2 days after transfection at a low density and treated with 1 mg/ml G418 sulfate (EMD Chemicals Inc., Gibbstown, NJ) for 2 weeks. Eight to 12 cell clones were chosen, expanded, and screened by western blotting. The clone having the highest expression level was then expanded to 10–15 plates of cells.

The cultured cells were incubated with 1 μ M 11-*cis*-retinal for 2 days and collected by centrifugation under dim red light. The collected cells were then incubated with 40 μ M 11-*cis*-retinal for 1 h at 4 °C via gentle rotation. The reconstituted visual pigments were extracted using 1% n-dodecyl β -D-maltoside (DDM) (Sigma-Aldrich, Saint Louis, MO) in 10 ml of extraction buffer (pH 6.7) (250 mM sucrose, 120 mM KCl, 10 mM MOPS, 5 mM MgCl₂, 1 mM DTT, 1 Roche protease inhibitor cocktail tablet) (Vought et al. 2000) via gentle rotation for 1 h at 4 °C. The visual pigments were then purified by immunoaffinity chromatography (Oprian et al. 1987). Briefly, the crude extract was slowly mixed with Sepharose beads conjugated with 1D4 IgG (University of British Columbia, Canada) overnight at 4 °C. The beads were then washed with 50 ml of wash buffer, pH 6.6 (20% glycerol, 120 mM KCl, 5 mM MgCl₂, 50 mM HEPES, and 0.1% DDM) (Vought et al. 2000). The visual pigments were eluted with 50 μ M competing peptide (Quality Controlled Biochemicals, Hopkinton, MA) in wash buffer and measured in a Hitachi U-3310 UV-Vis spectrophotometer at 0 °C. Spectral data represent the average of 5–8 scans. Estimates of λ_{max} were made by least-squares fitting of the data to a visual pigment template (Stavenga et al. 1993). For each construct, a minimum of $N = 3$ replicates were performed.

Drosophila Constructs, Fly Genetics, and Screening of Transformants

Transgenic fly lines were produced following the protocol of (Salcedo et al. 2003), except for the addition of the 1D4 epitope to the *BRh* opsin gene. A short sequence encoding 15 amino acids (STTVSKTETSQVAPA), inserted just before the stop codon, was placed under the control of the *Drosophila* Rh1 opsin promoter and introduced into the genome of *ninaE*¹⁷ mutant flies by P-element mediated germline transformation. Embryo injections were performed by BestGene, Inc., Chino Hills, CA or Genetic Services, Inc., Sudbury, MA. After homozygizing of the transformed lines, transgenic animals were screened for protein expression in the R1-6

photoreceptor cells by immunohistochemistry using the 1D4 antibody on cryostat-sectioned eyes and visualized using light microscopy. Genomic DNA was also extracted from individual fruit flies (one per transgenic line), and PCR-screened for the presence of the *Limenitis BRh* transgene. PCR products were sequenced to verify the identity of the transformant. The BRh visual pigment was purified from *Drosophila* eyes (Knox et al. 2003) and its absorbance spectra measured by 250–700 nm wavelength scans using a Hitachi U-3310 spectrophotometer at 15 °C.

Purification of *L. a. astyanax* Blue Rhodopsin from Transgenic *Drosophila*

Live *Drosophila* were kept in the dark overnight before snap freezing. Heads were separated from bodies under dim red light (Kodak #2 safelight filter) using dry ice and sieves (U.S. Standard stainless steel sieves #25 and #40, Fisher Scientific). All of the following procedures were carried out at 4 °C and under dim red light. Twenty-seven milliliters of heads were homogenized with a motorized Teflon homogenizer (MicroLux Power Tools, Micro-Mark) in 50 ml of homogenization buffer, pH 6.7 (250 mM sucrose, 120 mM KCl, 10 mM MOPS, 5 mM MgCl₂, 1 mM DTT, 10 µg/ml leupeptin, and 1.2 µg/ml pepstatin). The homogenate was centrifuged once at 1,000 × g for 10 min at 4 °C to remove the insoluble tissue. The supernatant was collected by centrifugation at 42,000 × g for 1 h at 4 °C (Sorvall RC-5B Refrigerated Superspeed Centrifuge, Dupont Instruments). The membrane pellet was homogenized with a Tissuemiser homogenizer (Fisher Scientific) for 5 s three times using the highest setting (30,000 rpm) in 50 ml of homogenization buffer containing 1% *N*-dodecyl-β-*D*-maltoside (LM), double foil wrapped, and slowly rotated at 4 °C overnight. The insoluble material was separated by centrifugation at 42,000 × g for 40 min at 4 °C. The supernatant was mixed with 300 µl of packed 1D4-Sepharose beads, double foil wrapped, and slowly rotated at 4 °C for 4 h. 1D4 IgG was obtained from University of British Columbia (Canada). Thirteen milliliters of wash buffer, pH 6.6 (20% glycerol, 120 mM KCl, 5 mM MgCl₂, 50 mM HEPES, 0.1% LM) was added to the tube containing the 1D4-Sepharose beads. The tube was then inverted 5–6 times and spun down gently in an International Clinical centrifuge (International Equipment Co.). This procedure was repeated four times. The rhodopsin was eluted with 450 µl of 40 µM competing peptide DEASTTVSKTETSQVAPA (Quality Controlled Biochemicals) in wash buffer and was concentrated to 70 µl using a C-10 Centricon tube (Amicon). The same amount of elution buffer was concentrated to 70 µl and used as the blank. The spectra of both blank and rhodopsin were measured by 650–250 nm wavelength scans using a Hitachi U-3310 spectrophotometer at room temperature. The rhodopsin was then illuminated with blue light using a narrow bandpass interference filter (442 nm, 10 nm full width-half maximum) (Edmund Optics) for 15 s and measured again. The 15-s irradiation treatment and spectral measurement was repeated two times. Finally, the rhodopsin was mixed with NH₂OH to a final concentration of 50 mM and the spectrum

was measured. All material was saved for western blot analysis.

Immunoblot Analysis

Immunoblotting was performed using standard techniques. Briefly, the purified rhodopsin samples (with OD₂₈₀~0.1) from the fly photochemistry experiments were prepared by diluting 1:100 in wash buffer (20% glycerol, 120 mM KCl, 5 mM MgCl₂, 50 mM HEPES, 0.1% LM, pH 6.6). Five microliters of the diluted protein samples, corresponding to approximately 3 heads of *Drosophila* expressing *L. a. astyanax* 1D4-BRh, were mixed with 5 µl 2 × Laemmli sample buffer (Bio-Rad Laboratories, Hercules, CA) and 1 µl 10% β-mercaptoethanol and shaken for 10 min on a Eppendorf Mixer 5,432 at 4 °C. Then, 11 µl protein sample and 10 µl PrecisionPlus Protein Dual Color Standard Ladder (Bio-Rad Laboratories) were loaded and separated on a 10% sodium dodecyl sulfate (SDS)–polyacrylamide electrophoresis gel (Invitrogen) on ice, and transferred to PVDF membranes (Invitrogen). The primary antibody used to probe the membrane for 2–4 h was mouse anti-1D4 IgG from University of British Columbia (Canada) in a dilution of 1:2,500 (5% milk powder in 1X PBT). The secondary antibody used was goat anti-mouse IgG-HRP (Santa Cruz Biotechnology) in a dilution of 1:1,000. Protein bands were visualized using enhanced chemiluminescence (Thermo Fisher Scientific, Rockford, IL) and exposure to film.

Optophysiology on Living *Drosophila*

Optophysiological measurements are based on microscopically monitoring the increase in scattering of light from photoreceptor cells of the fly eye that is due to rhodopsin-dependent physiological adaptation to bright illumination. As dark-adapted rhodopsin, a G protein-coupled receptor, is photoisomerized by light, Ca⁺⁺ levels increase in the photoreceptor cell, driving the migration of intracellular pigment granules toward the rhabdomere (reviewed in Stavenga 1995). This produces an increase in the scattering of light from the eye and a decrease in the amount of light stimulating the rhabdomere. The absorbance spectrum of the rhodopsin present in the photoreceptor cells can be estimated by measuring an action spectrum of this pupillary response, monitoring light scattering and adjusting the quantal intensity at each stimulus wavelength to create a criterion increase in reflectance. We used the double-beam epi-microspectrophotometer described in Briscoe and Bernard (2005) and the same procedures as described in Bernard and Stavenga (1979) for native flies to measure an optophysiological action spectrum for the *L. a. astyanax* 1D4-BRh rhodopsin expressed in adult *D. melanogaster ninaE¹⁷* flies. Briefly, a living adult fly was placed in a Plexiglas mount and the back of its head waxed to the Plexiglas to prevent head movement. The antennae were waxed together to keep arista away from the eye. The mount was then placed in the microspectrophotometer stage, and the fly was allowed to adapt to a steady, dim measuring beam (containing a broad-band orange filter, Hoya O56) passed through the microscope objective. Once

a stable preparation was achieved, ensuring that spontaneous eye movements were small, the experiment proceeded. Reflected light from the fly retina was measured following 10 s flashes of monochromatic light separated by a dark-interval of 99 s. Flash intensity was adjusted with a neutral density wedge until a 3% criterion increase in reflectance was reached. This procedure was repeated in a pseudorandom way every 10 nm at wavelengths ranging from 400 to 520 nm. After creating a satisfactory list of wavelengths and associated wedge settings, the fly was replaced by a calibrated Hamamatsu S1226-5BQ photodiode. Current produced by the photodiode was measured with a Keithley 616 nanoammeter, by obtaining the average of 12 automated runs for each setting in the list. To calculate sensitivity, we first used the manufacturer's responsivity curve to determine energy in units of nW. Normalized quanta (Q) were then calculated by dividing nW by wavelength, and normalized sensitivity was calculated as $1/Q$.

As a negative control, we attempted to measure an optophysiological response of the parental line of flies used for generating the transgenics for biochemistry, *ninaE*¹⁷. We confirmed that this fly, a mutant of *Drosophila Rh1*, that produces less than 1% *Rh1* mRNA compared with wild-type (O'Tousa et al. 1985), indeed lacks the optophysiological response that is typical of wild-type flies.

Epi-Microspectrophotometric Measurement of *L. a. astyanax* Blue-Absorbing Visual Pigment

A completely intact *L. a. astyanax* male was mounted in a slotted plastic tube, placed in the goniometric stage of the microspectrophotometer, oriented so the medio-ventral eye region (elevation = -20° , azimuth = 5°) was illuminated. The objective was focused inward to collapse all eyeshine to a small spot, and the field stop adjusted to mask that spot and exclude surrounding scattered light. The LWRh visual pigment R545 (Frentiu, Bernard, Cuevas, et al. 2007; Frentiu, Bernard, Sison-Mangus, et al. 2007) was bleached (Bernard 1983 a,b) from the rhabdoms by delivering 16 h of 3 s flashes every 60 s from a 45 watt illuminator filtered by a 3 mm Schott KG3 heat filter and an OG590 longpass filter. After a dark period of 28 min, the eyeshine reflectance spectrum was measured with dim monochromatic flashes of 5-nm bandwidth, from 380 to 750 nm every 10 nm. Densitometric analysis (see Materials and Methods in Briscoe et al. 2003, 2010; Yuan et al. 2010) revealed round-trip densities 0.30 of R545 and 0.32 of M490. Stripping R545 and M490 created a residual, fit by density 0.67 of R435. The normalized residual spectrum is shown in [supplementary figure S10B, Supplementary Material](#) online. The wavelength of peak absorbance (λ_{\max}) was estimated by least squares fit to the visual pigment template. Standard deviation of the fit was calculated in normalized absorbance units.

Statistical Analysis of Opsin SNP Frequencies

The effect of latitude on SNP frequencies was analysed using weighted logistic regressions for grouped data, with the glm function in R (R Core Team 2013). Logistic regression models

including both quadratic and linear terms were compared with models comprising linear terms only using Akaike information criterion (AIC) scores. Craig and Uhler's pseudo- R^2 , a logistic regression analog to R^2 obtained from linear regressions, was calculated using the pscl package in R (Zeileis et al. 2008).

AFLP Outlier Detection Analysis

Outlier analyses were run in BAYESCAN v. 2.0, with estimation of model parameters tuned automatically on the basis of short pilot runs (ten pilot runs, length 5,000), using default chain parameters: The sample size was set to 5,000 and the thinning interval to 20. Loci were then ranked according to their estimated posterior probability.

AMOVAs and Outlier Detection in Opsin Genes

AMOVA was performed for each of the five sequence data sets across the ten populations subdivided according to geographic sampling area. The data were partitioned into hierarchies of locally sampled demes and regional population groups (localities where only one of the *L. arthemis arthemis*, *L. a. astyanax* or intergrades occurs). Various AMOVA grouping schemes were examined to define the hierarchical groupings that best explained the highest proportion of the genetic variance. We computed final AMOVAs with 5,000 permutations, using pairwise differences to compute F_{ST} . To detect outlier SNPs potentially under selection, hierarchical island models (Excoffier et al. 2009) were implemented in Arlequin v. 3.5. The value of this approach over its predecessor (FDIST) (Beaumont and Nichols 1996) is that it better accounts for underlying population genetic structure in calculating F_{ST} and substantially reduces false positive rates in hierarchically structured populations (Excoffier et al. 2009). For these analyses, we grouped populations into several regional clusters to minimize differences among populations within groups, and used a 95% CI to identify outlier loci. We ran 100,000 iterations and simulated 100 demes per group for three groups with minimum and maximum expected heterozygosities bounded between 0 and 1 under a pairwise difference model.

Supplementary Material

Supplementary figures S1–S11 and tables S1–S8 are available at *Molecular Biology and Evolution* online (<http://www.mbe.oxfordjournals.org/>).

Acknowledgments

The authors thank Austin Platt and Fred Gagnon for butterflies, Anthony Long, Simon Blomberg, and Dimitrios Vagenas for advice on statistical analysis, and Daniel Osorio and J.J. Emerson for comments on the manuscript. The authors also thank Steven G. Britt, Phyllis Robinson, Julie Cridland, Saif Liswi, Rosalie Crouch, Cristina Cuevas, Emily Yee, Maita Kuvhenguwa, Anil Kumar, Steven Reppert, Xudong Qiu, David Berson, Nélica Pohl, and Deborah Jaworski for providing 11-*cis*-retinal, plasmids, technical advice, and support. The authors especially thank Bingnan Gu for suggesting that

stable HEK293 cell lines might improve protein expression levels and for his technical assistance with them. Sequence data have been deposited in Dryad under data identifier doi:10.5061/dryad.1r6c3. This work was supported by National Science Foundation grants DEB-1020136 to S.P.M and IOS-0819936, IOS-1025106 and DEB-1342759 to A.D.B.

References

- Antao T, Beaumont MA. 2011. Mcheza: a workbench to detect selection using dominant markers. *Bioinformatics* 27:1717–1718.
- Beaumont MA, Nichols RA. 1996. Evaluating loci for use in a genetic analysis of population structure. *Proc R Soc Lond B Biol Sci.* 263: 1619–1626.
- Benjamini Y, Hochberg Y. 1995. Controlling the false discovery rate: a practical and powerful approach to multiple testing. *J R Stat Soc S B.* 57:289–300.
- Bernard GD. 1983a. Bleaching of rhabdoms in eyes of intact butterflies. *Science* 219:69–71.
- Bernard GD. 1983b. Dark-processes following photoconversion of butterfly rhodopsins. *Biophys Struct Mech.* 9:277–286.
- Bernard GD, Stavenga DG. 1979. Spectral sensitivities of retinal cells measured in intact, living flies by an optical method. *J Comp Physiol.* 134:95–107.
- Berry A, Kreitman M. 1993. Molecular analysis of an allozyme cline: alcohol dehydrogenase in *Drosophila melanogaster* on the East Coast of North America. *Genetics* 134:869–893.
- Bierne N, Roze D, Welch JJ. 2013. Pervasive selection or is it. .? Why are FST outliers sometimes so frequent? *Mol Ecol.* 22:2061–2064.
- Briscoe AD, Bernard GD. 2005. Eyeshine and spectral tuning of long wavelength-sensitive rhodopsins: no evidence for red-sensitive photoreceptors among five Nymphalini butterfly species. *J Exp Biol.* 208: 687–696.
- Briscoe AD, Bernard GD, Szeto AS, Nagy LM, White RH. 2003. Not all butterfly eyes are created equal: rhodopsin absorption spectra, molecular identification, and localization of ultraviolet-, blue-, and green-sensitive rhodopsin-encoding mRNAs in the retina of *Vanessa cardui*. *J Comp Neurol.* 458:334–349.
- Briscoe AD, Bybee SM, Bernard GD, Yuan F, Sison-Mangus MP, Reed RD, Warren AD, Llorente-Bousquets J, Chiao CC. 2010. Positive selection of a duplicated UV-sensitive visual pigment coincides with wing pigment evolution in *Heliconius* butterflies. *Proc Natl Acad Sci U S A.* 107:3628–3633.
- Briscoe AD, Chittka L. 2001. The evolution of color vision in insects. *Annu Rev Entomol.* 46:471–510.
- Bybee SM, Yuan F, Ramstetter MD, Llorente-Bousquets J, Reed RD, Osorio D, Briscoe AD. 2012. UV photoreceptors and UV-yellow wing pigments in *Heliconius* butterflies allow a color signal to serve both mimicry and intraspecific communication. *Am Nat.* 179:38–51.
- Chiurugwi T, Beaumont MA, Wilkinson MJ, Battey NH. 2011. Adaptive divergence and speciation among sexual and pseudoviviparous populations in *Festuca*. *Heredity* 106:854–861.
- Coyne JA, Beecham E. 1987. Heritability of two morphological characters within and among natural populations of *Drosophila melanogaster*. *Genetics* 117:727–737.
- Cuevas JM, Domingo-Calap P, Sanjuan R. 2011. The fitness effects of synonymous mutations in DNA and RNA viruses. *Mol Biol Evol.* 19: 17–20.
- Endler JA. 1977. Geographic variation, speciation and clines. Princeton, New Jersey: Princeton University Press.
- Excoffier L, Hofer T, Foll M. 2009. Detecting loci under selection in a hierarchically structured population. *Heredity* 103:285–298.
- Excoffier L, Lischer HE. 2010. Arlequin suite ver 3.5: a new series of programs to perform population genetics analyses under Linux and Windows. *Mol Ecol Resour.* 10:564–567.
- Fabian DK, Kapun M, Nolte V, Kofler R, Schmidt PS, Schlotterer C, Flatt T. 2012. Genome-wide patterns of latitudinal differentiation among populations of *Drosophila melanogaster* from North America. *Mol Ecol.* 21:4748–4769.
- Finkbeiner SD, Briscoe AD, Reed RD. 2014. Warning signals are seductive: relative contributions of color and pattern to predator avoidance and mate attraction. *Heliconius* butterflies. *Evolution* 68: 3410–3420.
- Foll M, Gaggiotti O. 2008. A genome-scan method to identify selected loci appropriate for both dominant and codominant markers: a Bayesian perspective. *Genetics* 180:977–993.
- Frentiu FD, Bernard GD, Cuevas CI, Sison-Mangus MP, Prudic KL, Briscoe AD. 2007. Adaptive evolution of color vision as seen through the eyes of butterflies. *Proc Natl Acad Sci U S A.* 104: 8634–8640.
- Frentiu FD, Bernard GD, Sison-Mangus MP, Brower AVZ, Briscoe AD. 2007. Gene duplication is an evolutionary mechanism for expanding spectral diversity of the long wavelength photopigments of butterflies. *Mol Biol Evol.* 24:2016–2028.
- Frentiu FD, Briscoe AD. 2008. A butterfly eye's view of birds. *Bioessays* 30: 1151–1162.
- Frentiu FD, Chenoweth SF. 2010. Clines in cuticular hydrocarbons in two *Drosophila* species with independent population histories. *Evolution* 64:1784–1794.
- He Y, Vogelstein B, Velculescu VE, Papadopoulos N, Kinzler KW. 2008. The antisense transcriptomes of human cells. *Science* 322: 1855–1857.
- Hewitt G. 2000. The genetic legacy of the Quaternary ice ages. *Nature* 405:907–913.
- Hoffmann AA, Hallas R, Sinclair C, Mitrovski P. 2002. Opposing clines for high and low temperature resistance in *Drosophila melanogaster*. *Ecol Lett.* 5:614–618.
- Hut RA, Paolucci S, Dor R, Kyriacou CP, Daan S. 2013. Latitudinal clines: an evolutionary view on biological rhythms. *Proc Biol Sci.* 280: 20130433.
- Jacobs GH. 2012. The evolution of vertebrate color visions. *Adv Exp Med Biol.* 739:156–172.
- James AC, Azevedo RB, Partridge L. 1995. Cellular basis and developmental timing in a size cline of *Drosophila melanogaster*. *Genetics* 140:659–666.
- Knox BE, Salcedo E, Mathiesz K, Smith WC, Britt SG, Barlow RB. 2003. Heterologous expression of *Limulus* rhodopsin. *J Biol Chem.* 278: 40493–40502.
- Leather SR, Walters KF, Bale JS. 1993. The ecology of insect overwintering. Cambridge: Cambridge University Press.
- Lucas PW, Dominy NJ, Riba-Hernandez P, Stoner KE, Yamashita N, Loria-Calderón E, Petersen-Pereira W, Rojas-Durán Y, Salas-Pena R, Solis-Madrigo S, et al. 2003. Evolution and function of routine trichromatic vision in primates. *Evolution* 57:2636–2643.
- Lythgoe JN. 1979. The ecology of vision. Oxford, U.K.: Clarendon Press.
- Mercer TR, Dinger ME, Mattick JS. 2009. Long non-coding RNAs: insights into functions. *Nat Rev Genet.* 10:155–159.
- Mullen SP, Dopman EB, Harrison RG. 2008. Hybrid zone origins, species boundaries, and the evolution of wing-pattern diversity in a polytypic species complex of North American admiral butterflies (Nymphalidae: *Limenitis*). *Evolution* 62:1400–1417.
- Mullen SP, Savage WK, Wahlberg N, Willmott KR. 2011. Rapid diversification and not clade age explains high diversity in neotropical *Adelpha* butterflies. *Proc Biol Sci.* 278:1777–1785.
- Nathans J. 1990. Determinants of visual pigment absorbance: identification of the retinylidene Schiff's base counterion in bovine rhodopsin. *Biochemistry* 29:9746–9752.
- Opryan DD, Molday RS, Kaufman RJ, Khorana HG. 1987. Expression of a synthetic bovine rhodopsin gene in monkey kidney cells. *Proc Natl Acad Sci U S A.* 84:8874–8878.
- O'Tousa JE, Baehr W, Martin RL, Hirsh J, Pak WL, Applebury ML. 1985. The *Drosophila ninaE* gene encodes an opsin. *Cell* 40: 839–850.
- Palacios AG, Goldsmith TH, Bernard GD. 1996. Sensitivity of cones from a cyprinid fish (*Danio aequipinnatus*) to ultraviolet and visible light. *Vis Neurosci.* 13:411–421.

- Partridge L, Barrie B, Fowler K, French V. 1994. Evolution and development of body size and cell size in *Drosophila melanogaster* in response to temperature. *Evolution* 48:1269–1276.
- Pohl N, Sison-Mangus MP, Yee EN, Liswi SW, Briscoe AD. 2009. Impact of duplicate gene copies on phylogenetic analysis and divergence time estimates in butterflies. *BMC Evol Biol.* 9:99.
- R Core Team. 2013. A language and environment for statistical computing. Vienna, Austria: R Foundation for Statistical Computing.
- Salcedo E, Zheng L, Phistry M, Bagg EE, Britt SG. 2003. Molecular basis for ultraviolet vision in invertebrates. *J Neurosci.* 23:10873–10878.
- Sandrelli F, Tauber E, Pegoraro M, Mazzotta G, Cisotto P, Landskron J, Stanewsky R, Piccin A, Rosato E, Zordan M, et al. 2007. A molecular basis for natural selection at the *timeless* locus in *Drosophila melanogaster*. *Science* 316:1898–1900.
- Sauman I, Briscoe AD, Zhu H, Shi D, Froy O, Stalleicken J, Yuan Q, Casselman A, Reppert SM. 2005. Connecting the navigational clock to sun compass input in the monarch fly brain. *Neuron* 46:457–467.
- Schmidt PS, Matzkin L, Ippolito M, Eanes WF. 2005. Geographic variation in diapause incidence, life-history traits and climatic adaptation in *Drosophila melanogaster*. *Evolution* 59:1721–1732.
- Schmidt PS, Zhu C-T, Das J, Batavia M, Yang L, Eanes WF. 2008. An amino acid polymorphism in the *couch potato* gene forms the basis for climatic adaptation in *Drosophila melanogaster*. *Proc Natl Acad Sci U S A.* 105:16207–16211.
- Schnall-Levin M, Zhao Y, Perrimon N, Berger B. 2010. Conserved microRNA targeting in *Drosophila* is as widespread in coding regions as in 3'UTRs. *Proc Natl Acad Sci U S A.* 107:15751–15756.
- Seehausen O, Terai Y, Magalhaes IS, Carleton KL, Mrosso HD, Miyagi R, van der Sluijs I, Schneider MV, Maan Tachida H, Imai H, et al. 2008. Speciation through sensory drive in cichlid fish. *Nature* 455:457–467.
- Shabalina SA, Spiridonov NA, Kashina A. 2013. Sounds of silence: synonymous nucleotides as a key to biological regulation and complexity. *Nucleic Acids Res.* 41:2073–2094.
- Shen WL, Kwon Y, Adegbola AA, Luo J, Chess A, Montell C. 2011. Function of rhodopsin in temperature discrimination in *Drosophila*. *Science* 331:1333–1336.
- Shields DC, Sharp PM, Higgins DG, Wright F. 1988. "Silent" sites in *Drosophila* genes are not neutral: evidence of selection among synonymous codons. *Mol Biol Evol.* 5:704–716.
- Stalleicken J, Labhart T, Mouritsen H. 2006. Physiological characterization of the compound eye in monarch butterflies with focus on the dorsal rim area. *J Comp Physiol A.* 192:321–331.
- Stavenga DG. 1995. Insect retinal pigments: spectral characteristics and physiological functions. *Prog Retin Eye Res.* 15:231–259.
- Stavenga DG, Smits RP, Hoenders BJ. 1993. Simple exponential functions describing the absorbance bands of visual pigment spectra. *Vision Res.* 33:1011–1017.
- Terakita A, Yamashita N, Shichida Y. 2000. Highly conserved glutamic acid in the extracellular IV-V loop in rhodopsins acts as the counter-ion in retinochrome, a member of the rhodopsin family. *Proc Natl Acad Sci U S A.* 97:14263–14267.
- van Heerwarden B, Lee RF, Wegener B, Weeks AR, Sgrò CM. 2012. Complex patterns of local adaptation in heat tolerance in *Drosophila simulans* from eastern Australia. *J Evol Biol.* 25:1765–1778.
- Vought BW, Salcedo E, Chadwell LV, Britt SG, Birge RR, Knox BE. 2000. Characterization of the primary photointermediates of *Drosophila* rhodopsin. *Biochemistry* 39:14128–14137.
- Wakakuwa M, Terakita A, Koyanagi M, Stavenga DG, Shichida Y, Arikawa K. 2010. Evolution and mechanism of spectral tuning of blue-absorbing visual pigments in butterflies. *PLoS One* 5:e15015.
- Yokoyama S. 2002. Molecular evolution of color vision in vertebrates. *Gene* 300:69–78.
- Yuan F, Bernard GD, Le J, Briscoe AD. 2010. Contrasting modes of evolution of the visual pigments in *Heliconius* butterflies. *Mol Biol Evol.* 27:2392–2405.
- Zeileis A, Kleiber C, Jackman S. 2008. Regression models for count data in R. *J Stat Soft.* 27:8.